Nuclear Physics B82 (1974) 201–212. North-Holland Publishing Company

ELECTROEXCITATION OF NUCLEON RESONANCES ON PROTONS AND NEUTRONS

M. KÖBBERLING, J. MORITZ, K.H. SCHMIDT, D. WEGENER* and D. ZELLER
Insitut für Experimentelle Kernphysik der Universität und des Kernforschungszentrums Karlsruhe

J. BLECKWENN
Deutsches Elektronensynchrotron DESY, Hamburg

F.H. HEIMLICH
Fakultät für Physik der Universität, Freiburg

Received 27 July 1974

Abstract: New data for the total absorption cross section of virtual photons on protons and deuterons are used to determine the excitation cross section of the three dominant nucleon resonances at W = 1236 MeV, W = 1520 MeV and W = 1685 MeV. The q^2 dependence of the excitation on protons and of the ratio for the excitation on deuterons and protons is given. The results are compared with the predictions of the symmetric quark model.

1. Introduction

The absorption cross section of virtual photons on protons and neutrons for four-momentum transfers 0.1 $(\mathrm{GeV}/c)^2 \leqslant q^2 \leqslant 1.5\ (\mathrm{GeV}/c)^2$ and invariant masses $W \leqslant 1.85$ GeV has been determined by the Karlsruhe-DESY collaboration. The experiment has been performed with a wire spark chamber spectrometer, using a Čerenkov counter and a shower counter for particle identification. The details of the apparatus have been described in former publications [1, 3]. The measured cross section, the corrections and the error sources are given in tabulated form in a previous paper [4]. In the present paper the contribution of the dominant nucleon resonances and the non-resonant background to the measured and radiatively corrected cross section is determined.

* Present address: CERN, Geneva.

2. Analysis procedure and results

The measured two-fold differential cross section is connected to the absorption cross section σ_{tot} by

$$\sigma_{tot} = \sigma_T + \epsilon \sigma_L = \frac{1}{\Gamma_T} \frac{d^3\sigma}{d\Omega dE},$$

where ϵ is the degree of transverse polarization of the virtual photons, Γ_T is the flux of virtual photons. σ_T and σ_L are the absorption cross sections of transverse respectively longitudinal polarized virtual photons.

The resonance cross sections are derived from the absorption cross section on protons and deuterons in two steps. By fitting of the resonance and the background contributions to the proton data the resonance parameters were determined. To get the resonance contribution from the deuteron cross section the Fermi motion was taken into account.

The resonance contributions to the absorption cross section were parametrized by Breit-Wigner formulas. For the $\Delta(1236)$ resonance a relativistic Breit-Wigner formula with mass dependent width was chosen [3]:

$$\sigma_{1236} = \frac{\pi\alpha q^2}{2KWM} \frac{\Gamma(W)}{(W-M_1^*)^2 + \frac{1}{4}\Gamma^2(W)} G_M^{*2}(q^2), \tag{1}$$

$$\Gamma(W) = \frac{0.128\,(0.85|p_\pi^*|/m_\pi)^3}{1 + (0.85\,|p_\pi^*|\,/m_\pi)^2}, \tag{2}$$

where M_1^* is the resonance mass, q the three-momentum of the virtual photon, W the invariant mass of the hadronic final state, $G_M^*(q^2)$ the transition form factor, α the fine structure constant, K the equivalent photon energy, p_π^* the pion momentum in the c.m. system of the resonance and m_π the pion mass.

The second and third nucleon resonances are described by nonrelativistic Breit-Wigner formulas.

$$\sigma_{1520} = A_2(q^2) \frac{\Gamma(1520)}{(W-M_2^*)^2 + \frac{1}{4}\Gamma^2(1520)}, \tag{3}$$

$$\sigma_{1685} = A_3(q^2) \frac{\Gamma(1685)}{(W-M_3^*)^2 + \frac{1}{4}\Gamma^2(1685)}. \tag{4}$$

To fit the non-resonant background a polynomial was used

$$\sigma_{nres} = \sum_{n=1}^{N} a_n(q^2)\,(W-W_{th})^{n-\frac{1}{2}}, \tag{5}$$

where the square root term $(W-W_{th})^{\frac{1}{2}}$ takes into account the behaviour of non-res-

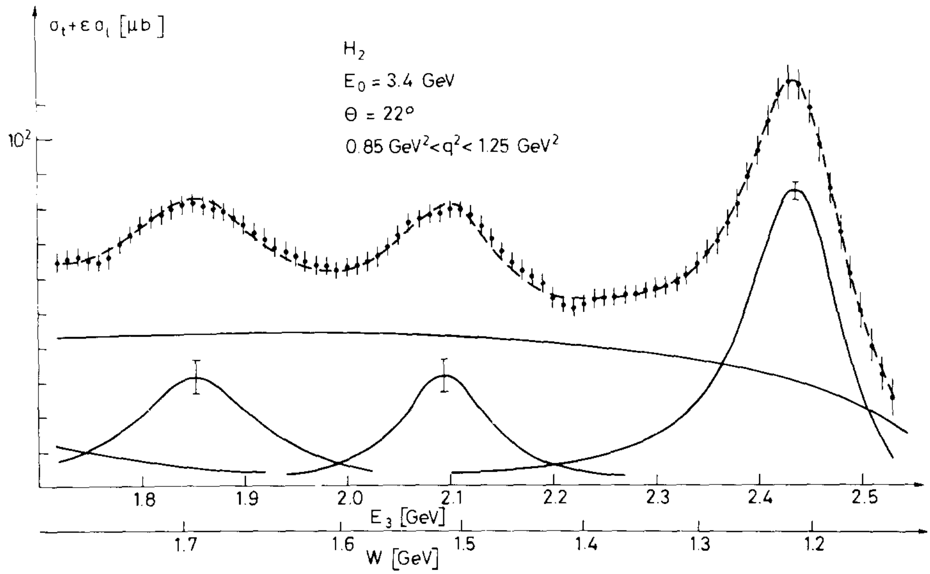

Fig. 1. Separation of resonant and non-resonant contribution of a measured electron spectrum using a proton target.

onant pion production at the threshold W_{th}. The value $N = 3$ gives a sufficient fit and has been used throughout the analysis. Values $N > 3$ have been tried, but they do not give significant different results.

The fit to the proton data leads to the following set of resonance parameters:

$M_1^* = 1.222 \pm 0.005$ GeV,

$M_1^* = 1.51 \pm 0.008$ GeV, $\Gamma(1520) = 0.08$ GeV ,

$M_1^* = 1.685 \pm 0.014$ GeV, $\Gamma(1685) = 0.1$ GeV .

This result agrees with the analysis of Bloom et al. [5] at higher four-momentum transfers. An example of the fit to the measured proton cross sections is given in fig. 1. In fig. 2 the resonance cross sections of the proton as a function of the four-momentum transfer are given. The results are summarized in table 1 and table 2.

To compare the excitation cross section of resonances on bound state protons with that one on bound state neutrons we have folded the cross section of the free proton with the momentum distributions of the nucleons bound in the deuteron

$$\frac{d^2\sigma}{d\Omega_3 dE_3}(E_1, E_3, \theta) = \int d^3p \left\{ W(\boldsymbol{p})\, F(\boldsymbol{p}) \frac{d^2\sigma_0(E_1^*, E_3^*, \theta^*)}{d\Omega_3^* dE_3^*} \frac{dE_3^*}{dE_3} \frac{d\Omega_3^*}{d\Omega_3} \right\}, \tag{6}$$

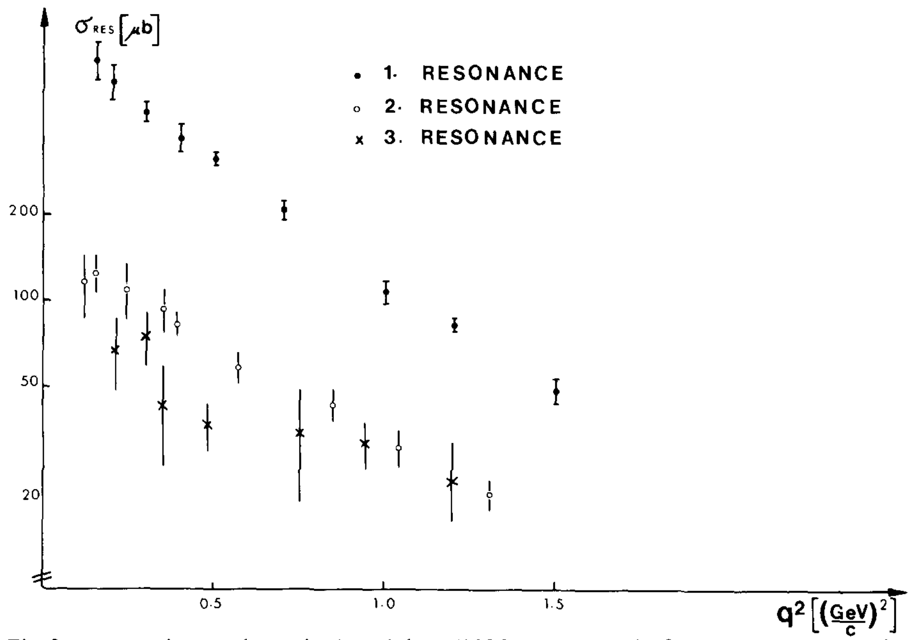

Fig. 2. Cross section for the excitation of the Δ(1236) resonance, the 2nd resonance and the 3rd resonance as a function of the four-momentum transfer q^2.

where in the lab frame $\boldsymbol{p}$ is the momentum of the target nucleon, E_1 the energy of the primary electron, E_3 the energy of the scattered electron and θ the scattering angle of the electron.

The kinematic variables measured in the rest system of the target nucleons are

Table 1
Transition form factor $G_M^*(q^2)$ for the excitation of the Δ(1236) resonance on protons and neutrons

q^2 (GeV/c)^2	G_{Mp}^*	G_{Mn}^*
0.15	2.15 ± 0.13	
0.20	1.79 ± 0.12	1.76 ± 0.15
0.30	1.38 ± 0.04	1.28 ± 0.10
0.40	1.10 ± 0.08	1.02 ± 0.08
0.50	0.92 ± 0.03	0.91 ± 0.04
0.70	0.64 ± 0.02	0.60 ± 0.03
1.0	0.39 ± 0.02	0.36 ± 0.03
1.2	0.31 ± 0.01	0.31 ± 0.02
1.5	0.22 ± 0.01	0.21 ± 0.02

Table 2a
Excitation cross section of the $\Delta(1236)$ resonance on protons

q^2 (GeV/c)^2	$\sigma_T + \epsilon\sigma_L$ (μb)
0.15	690 ± 100
0.20	580 ± 80
0.30	460 ± 30
0.40	370 ± 40
0.50	315 ± 15
0.70	210 ± 15
1.0	110 ± 10
1.2	85 ± 5
1.5	50 ± 5

Table 2b
Excitation cross section of the 2nd nucleon resonance on protons

q^2 (GeV/c)^2	$\sigma_T + \epsilon\sigma_L$ (μb)
0.12	116 ± 30
0.15	126 ± 20
0.24	110 ± 24
0.34	94 ± 16
0.39	84 ± 7
0.57	59 ± 7
0.84	44 ± 6
1.04	31 ± 5
1.32	22 ± 3

Table 2c
Excitation cross section of the 3rd nucleon resonance on protons

q^2 (GeV/c)^2	$\sigma_T + \epsilon\sigma_L$ (μb)
0.21	68 ± 20
0.30	75 ± 16
0.33	43 ± 17
0.48	37 ± 7
0.74	35 ± 15
0.93	32 ± 6
1.20	24 ± 9

characterized by an asterisk. $W(\boldsymbol{p})$ is the momentum distribution of the target nucleons. It is calculated from the Fourier transform of the Hulthen wave function (5% d-state contribution). By the term $F(\boldsymbol{p})$ we take into account the influence of the movement of the target nucleons to the flux of the virtual photons. To solve the inte gral equation (6) the following representation of the two-fold differential cross section is used:

$$\frac{d^2\sigma}{d\Omega_3 dE_3} = \sigma_{\rm Mott}\ \{W_2(q^2,\nu) + 2{\rm tg}^2\tfrac{1}{2}\theta\ W_1(q^2,\nu)\} \equiv \sigma_{\rm Mott} f(\nu, q^2, \theta)\ . \tag{7}$$

Merging of (7) into (6) results in

$$\frac{d^2\sigma}{d\Omega_3 dE_3}(E_1, E_3, \theta) = \sigma_{\rm Mott}(E_1, E_3, \theta) \int d^3p\ \{W(\boldsymbol{p}) f(\nu^*, q^2, \theta^*)$$

$$\times (1 - p_x \sin\theta - p_z \cos\theta)^2\}, \tag{8}$$

$$\nu^* = E_1^* - E_3^*\ , \tag{9}$$

$$E_1^* = E_1 (1 - p_z)\ , \tag{10}$$

$$E_3^* = E_3 (1 - p_x \sin\theta - p_z \cos\theta). \tag{11}$$

The direction of the primary electron beam is taken as z-axis, while the x-axis is placed in the electron scattering plane ($\hbar = c = M = 1$).

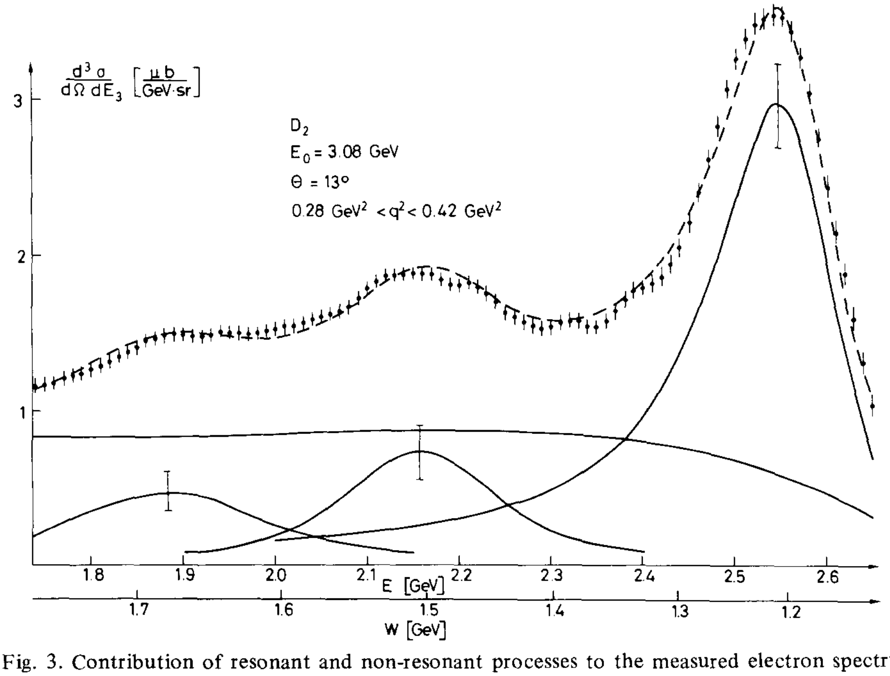

Fig. 3. Contribution of resonant and non-resonant processes to the measured electron spectrum for deuteron targets.

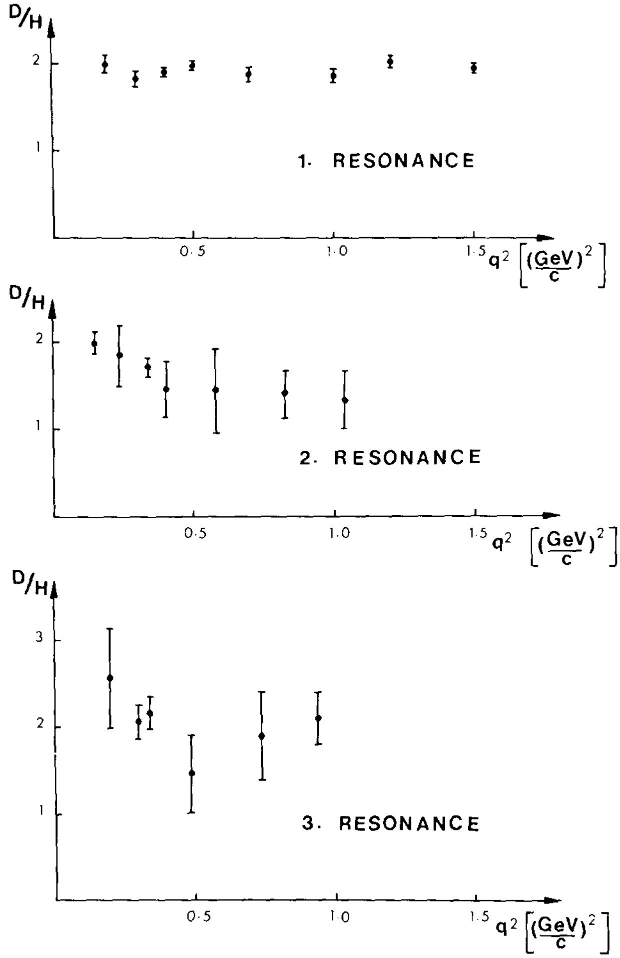

Fig. 4. Ratio of the cross section for the resonance excitation on deuterons and protons as a function of the four-momentum transfer.

From formula (8) follows that the folding procedure consists in a superposition of cross sections at constant q^2 and different ν^*. At small electron scattering angles an energy interval proportional to ν contributes to the broadening, therefore the resonances with high masses are broadened strongest. The function $f(\nu^*, q^2, \theta^*)$ in formula (8) was determined by interpolation from the experimental values given in ref. [4]

This folding procedure has been applied separately to each of the resonant contributions determined from the proton cross sections. The folded resonance contributions and the Fermi-broadened background

$$\sigma_D = a_1\sigma_f(1236) + a_2\sigma_f(1520) + a_3\sigma_f(1680) + a_4\sigma_f(\text{nres}) \qquad (12)$$

Table 3a
Ratio σ_D/σ_p of cross sections for the excitation of the Δ (1236) resonance on deuterons and protons

q^2 (GeV/c)^2	σ_D/σ_p
0.20	1.99 ± 0.1
0.30	1.82 ± 0.1
0.40	1.87 ± 0.05
0.50	1.96 ± 0.05
0.70	1.88 ± 0.07
1.0	1.86 ± 0.08
1.2	2.02 ± 0.1
1.5	1.93 ± 0.05

Table 3b
Ratio σ_D/σ_p of cross sections for the excitation of the 2nd resonance on deuterons and protons

q^2 (GeV/c)^2	σ_D/σ_p
0.15	2.00 ± 0.15
0.24	1.85 ± 0.35
0.34	1.72 ± 0.12
0.39	1.48 ± 0.3
0.57	1.45 ± 0.5
0.84	1.4 ± 0.3
1.04	1.35 ± 0.35

Table 3c
Ratio σ_D/σ_p of cross sections for the excitation of the 3rd resonance on deuterons and protons

q^2 (GeV/c)^2	σ_D/σ_p
0.21	2.55 ± 0.6
0.30	2.05 ± 0.2
0.33	2.15 ± 0.2
0.48	1.45 ± 0.45
0.74	1.9 ± 0.5
0.93	2.1 ± 0.3

have been fitted to the measured deuteron cross sections. Fig. 3 shows an example of a fit for a deuterium target.The constants $a_1, ..., a_4$ have been determined by the fit. The ratio of the single resonance term to the appropriate proton term in the maximum of the resonance measures the resonance excitation on neutrons. Corrections due to shadowing and the Pauli principle are less than 6% and decreases with increasing four-momentum transfer. Therefore no corrections of this kind have been applied to the data. Fig. 4 shows the ratio of resonance excitation on deuterons and protons as a function of the four-momentum transfer in the region of the three-nucleon resonances. These results are given in table 3.

3. Discussion of the results

The excitation of the Δ(1236) resonance on protons and neutrons is characterized by the transition form factor $G_M^*(q^2)$ of formula (1). The results of the present analysis are given in fig. 5. Since only the isovector amplitude contributes to this transition form factor, the excitation of the Δ(1236) resonance on protons and neutrons should be equal. This result is in agreement with a former experiment which was performed in a smaller q^2 region [6].

The prediction of the dispersion relation model of Gutbrod and Simon [14] included in fig. 5, fits the experimental data. A dipole like formula has been fitted to the transition form factor:

$$G_M^*(q^2) = \frac{\mu^*}{(1+q^2/0.51)^2}, \tag{13}$$

where q^2 is measured in $(\text{GeV}/c)^2$. The transition moment

$$\mu^* = 3.54 \pm 0.4,$$

determined from the fit is in agreement with results from photoproduction [7].

Theoretical results for the excitation of higher nucleon resonances have been given by Ravndal [8] and Lipes [9] in a relativistic version of the symmetric quark model. In figs. 6 and 7 the theoretical prediction and the experimental results for the proton target are compared. The q^2 dependence and the strength of the measured cross section deviate from the predictions of the two models.

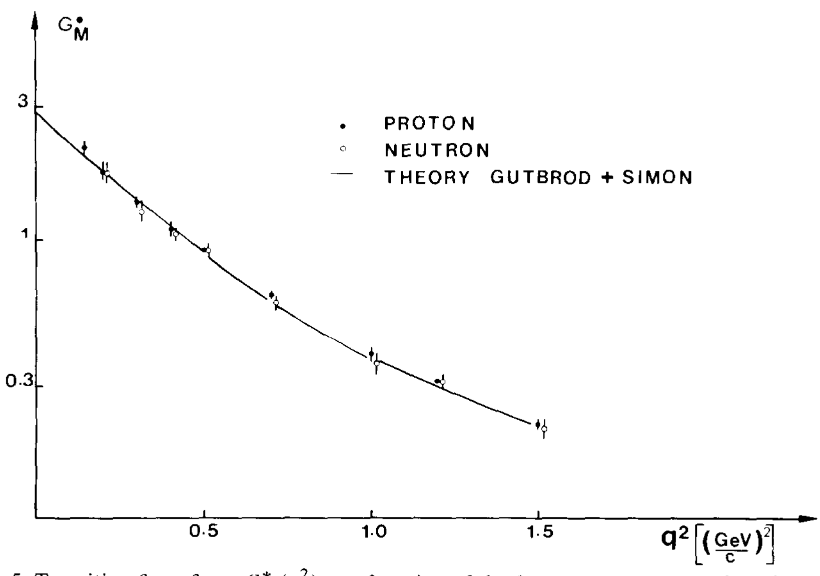

Fig. 5. Transition form facor $G_M^*(q^2)$ as a function of the four-momentum transfer. The solid line is the prediction of Gutbrod and Simon [14].

As fig. 6 shows, the differences between the Ravndal model and the data for the excitation cross section of the 2nd resonance is due to the large longitudinal cross section predicted by this model. Since the excitation of the S_{11} (1535) resonance is described satisfactorily by the Lipes version of the symmetric quark model [10, 11] one has to conclude that the theory of Lipes and the experiment differ mainly for the D_{13} (1512) resonance contribution.

The maximum of the resonance in the region of the 3rd resonance is shifted to higher invariant masses with increasing four momentum transfer [4]. This trend is in agreement with the quark model predictions and supports the calculations which determine the contributions of the different nucleon resonances to the measured cross section. But fig. 7 demonstrates that in the detailed shape of the q^2 dependence and the absolute height of the cross-section theory and experiment disagree. From this follows that the symmetric quark model, which is successful in photoproduction [12] is only of limited predictive power in electroproduction. This is most probable due to the fact that the q^2 dependence of the cross section is strongly affected by the quark wave function chosen.

Close et al. [13] have derived upper and lower limits for the ratio σ_N/σ_P of the excitation cross section of nucleon resonances on neutrons and protons which can be used to determine the ratio σ_D/σ_P of the cross sections for resonance excitation on deuterons and protons. They have taken into account the difference between constituent and current quarks by classifying the nucleon resonances according to $SU(6)_W$

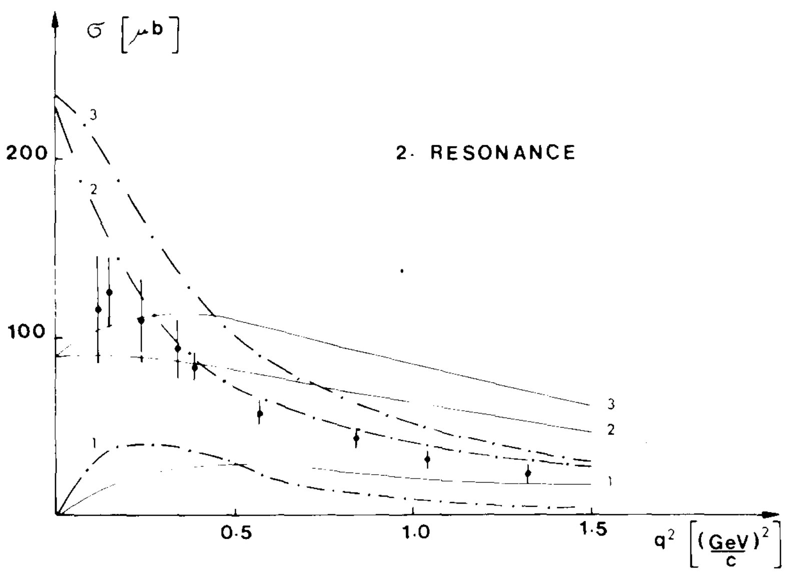

Fig. 6. Cross section for the excitation of resonances on protons in the region of the 2nd resonance as a function of the four-momentum transfer. For comparison the predictions of Ravndal [8] (——) and Lipes [9] (–·–·–) are included: (1) σ_l; (2) σ_t; (3) $\sigma_t + \epsilon\sigma_l$.

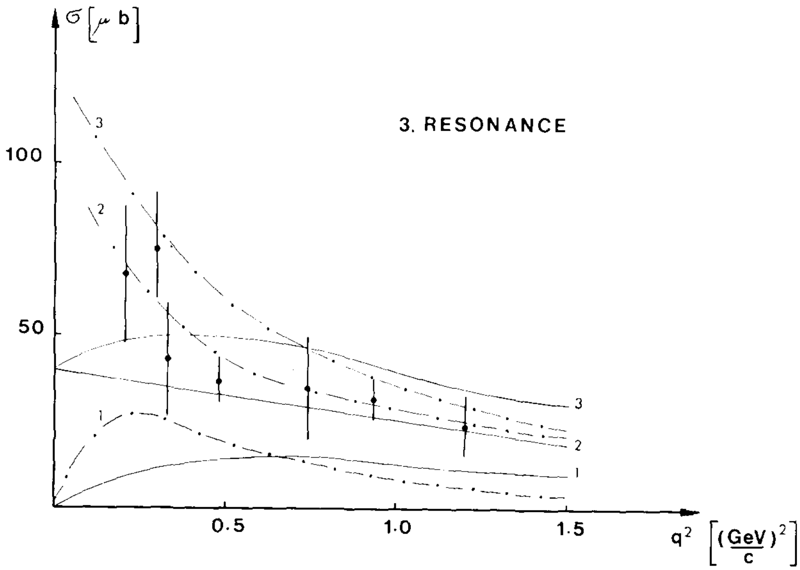

Fig. 7. Cross section for the excitation of resonances on protons in the region of the 3rd resonance as a function of the four-momentum transfer. For comparison the theoretical predictions of Ravndal [8] (——) and Lipes [9] (·–·–) are included; (1) σ_l; (2) σ_t; (3) $\sigma_t + \epsilon\sigma_l$.

in the constituent basis. Furthermore they used the most general form for the current which is compatible with it belonging to a 35-plet of $SU(6)_W$. Without any further assumptions on the quark wave function upper and lower limits for the ratio σ_D/σ_P of the different nucleon resonances can be derived from their calculations.

In the region of the 2nd resonance the limits are given by $0 \leqslant \sigma_D/\sigma_P \leqslant 2$ dependent on the contribution of the known three nucleon resonances in this mass interval. As shown by fig. 4b this prediction is compatible with the results of the present analysis.

In the region of the 3rd resonance, the model predicts for the $S_{31}(1650)$ and the $D_{33}(1670)$ resonance a ratio $\sigma_D/\sigma_P = 2$. The $D_{15}(1670)$ resonance should not be excited on protons and for the $F_{15}(1688)$ resonance the limit for the ratio is $0 \leqslant \sigma_D/\sigma_P \leqslant 4/9$. The results of fig. 4c are compatible with this model either if the $S_{31}(1650)$ and the $D_{33}(1670)$ resonance dominate the excitation cross section or if the $D_{15}(1670)$ and the $F_{15}(1688)$ resonance are excited with equal strength.

In conclusion it follows that the general results of the quark model are in good agreement with the experimental data, while specific theoretical predictions, which depend sensitively on the wave function chosen, differ from the experimental results.

The help of Ing. H. Sindt during all stages of the experiment is acknowledged. This work has been supported by the Bundesministerium für Forschung und Technologie.

References

[1] J. Moritz, K.H. Schmidt, D. Wegener, J. Bleckwenn and E. Engels Jr., Nucl. Phys. B41 (1972) 336.
[2] J. Bleckwenn, H. Klein, J. Moritz, K.H. Schmidt and D. Wegener, Nucl. Phys. B33 (1971) 475.
[3] S. Galster, G. Hartwig, H. Klein, J. Moritz, K.H. Schmidt, W. Schmidt-Parzefall, D. Wegener and J. Bleckwenn, Phys. Rev. D5 (1972) 519.
[4] M. Köbberling, J. Moritz, K.H. Schmidt, D. Wegener, D. Zeller, J. Bleckwenn and F.H. Heimlich, Kernforschungszentrum Karlsruhe, KFK-Bericht 1822 (1973).
[5] W.K.H. Panofsky, 14th Int. Conf. on high-energy physics, Vienna 1968, p. 23;
E. Bloom, D. Coward, H. De Staebler, J. Drees, J. Litt, G. Miller, L. Mo, R.E. Taylor, M. Breidenbach, J.I. Friedman, H.W. Kendall and S. Loken, paper presented to the 14th Int. Conf. on high-energy physics, Vienna, 1968;
M. Breidenbach, 1970 PhD thesis LNS-MIT 2098-635 PhD thesis, MIT.
[6] J. Bleckwenn, J. Moritz, K.H. Schmidt and D. Wegener, Phys. Letters 38B (1972) 265.
[7] G. Ebel, A. Müllensiefen, H. Pilkuhn, F. Steiner, D. Wegener, M. Gourdin, C. Michael, J.L. Peterson, M. Roos, B.R. Martin, G. Oades and J.J. De Swart, Nucl. Phys. B33 (1971) 317.
[8] R.P. Feynman, M. Kislinger and F. Ravndal, Phys. Rev. D3 (1971) 2706;
F. Ravndal, Phys. Rev. D4 (1971) 1466.
[9] R.G. Lipes, Phys. Rev. D5 (1972) 2849.
[10] P.S. Kummer, E. Ashburner, F. Foster, G. Hughes, R. Siddle, J. Allison, B. Dickinson, E. Evangelides, M. Ibbotson, R.S. Lawson, R.S. Meaburn, H.E. Montgomery and W.J. Schuttleworth, Phys. Rev. Letters 30 (1973) 873.
[11] U. Beck, K.H. Becks, V. Burkert, J. Drees, G. Knop, H. Kolanoski, M. Leenen, K. Moser, Ch. Nietzel, J. Päsler, K. Rith, R. Sauerwein, E. Schlösser and H.E. Stier, Bonn preprint, PIB 1-217 (August 1973).
[12] J.K. Walker, Proc. of Int. Symp. on electron and photon interactions at high energies, Liverpool, 1969.
[13] F.E. Close, H. Osborn and A.M. Thomson, CERN preprint 1818 (February 1974).
[14] F. Gutbrod and D. Simon, Nuovo Cimento 51A (1967) 602.